Int. J. Urban Manage. Energy Sustainability, 6(4):353-365, 2025

International Journal of Urban Management and Energy Sustainability (IJUMES)

Homepage: http://www.ijumes.com

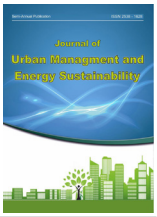

CASE STUDY RESEARCH PAPER

Laboratory Analysis of the Hydrodynamic Behaviour of Perforated Breakwaters Constructed from Recycled Materials

Jamil Ahmadi[1], Mohammad Hadi Tavana[2*], Ehsan Delavari[1], Shamsa Basirat[1]

1 Department of Civil Engineering, Na.C., Islamic Azad University, Isfahan, Iran

*2*Department of Civil Engineering, Ker.C., Islamic Azad University, Kermanshah, Iran*

ARTICLE INFO

Article History:
Received 2025-08-25
Revised 2025-10-20
Accepted 2025-12-03

Keywords:
Laboratory modelling; perforated breakwater; recycled materials; wave reflection; wave transmission

ABSTRACT

Population growth and intensive development along coastlines have increased the demand for effective, low-cost and environmentally responsible coastal-protection structures. Problem statement: Conventional rock and concrete breakwaters consume large volumes of natural resources, impose high construction costs and disrupt near-shore water circulation and sediment transport; a permeable alternative that dissipates wave energy while preserving water exchange is therefore needed, particularly for the ports and waterways of Iran's southern coasts along the Persian Gulf. Aim: This study analyses, through physical modelling, the hydrodynamic behaviour of perforated breakwaters built from recycled materials and identifies the configuration that best combines wave attenuation with structural stability. Methodology: Physical models with single-row, double-row, double-sided, horizontal and vertical arrangements were tested in a wave flume at a 1:13 scale under regular waves. Perforations of varying number and diameter were introduced on the front and rear faces, and the reflection coefficient, run-up, transmission coefficient, uplift force and overturning moment were measured. Findings: The perforations effectively dissipated wave energy and reduced reflection, transmission, uplift and overturning moments. Horizontal perforated breakwaters near the water surface experienced lower uplift. Increasing the perforation percentage from 7% to 42.78% raised energy dissipation and lowered run-up, whereas increasing it further to 78.5% reversed the trend; the 42.78% configuration minimised wave transmission. Conclusion: The best overall performance was obtained with the two-row, double-sided breakwater in a combined wave-facing arrangement, which showed minimal displacement and the greatest stability, confirming perforated breakwaters made from recycled materials as a sustainable and effective coastal-protection option.

DOI: 10.22034/ijumes.2026.2097984.1396

Running Title: Laboratory Analysis of the Hydrodynamic Behavior of Perforated Breakwaters Constructed

NUMBER OF REFERENCES	NUMBER OF FIGURES	NUMBER OF TABLES
40	09	03

*Corresponding Author:
Email: *M.H.Tavana@iau.ac.ir*
Phone: 00988337243181
ORCID: https://orcid.org/0000-0001-6785-7840

INTRODUCTION

Rapid advances in marine science and the increasing population density of coastal areas have intensified the need for effective coastal-protection solutions. Coastal regions along the Persian Gulf are particularly vulnerable to wave-induced erosion, sediment movement and shoreline degradation. Traditional breakwaters constructed from massive rock or concrete units require extensive natural resources and impose high construction costs. Consequently, sustainable approaches such as permeable breakwaters and the use of recycled materials have gained increasing attention (Kenny & Rozovsky, 2023; Moradi & Shahnoori, 2021). The geographical setting of the study is shown in Figure 1. (Fig. 1)

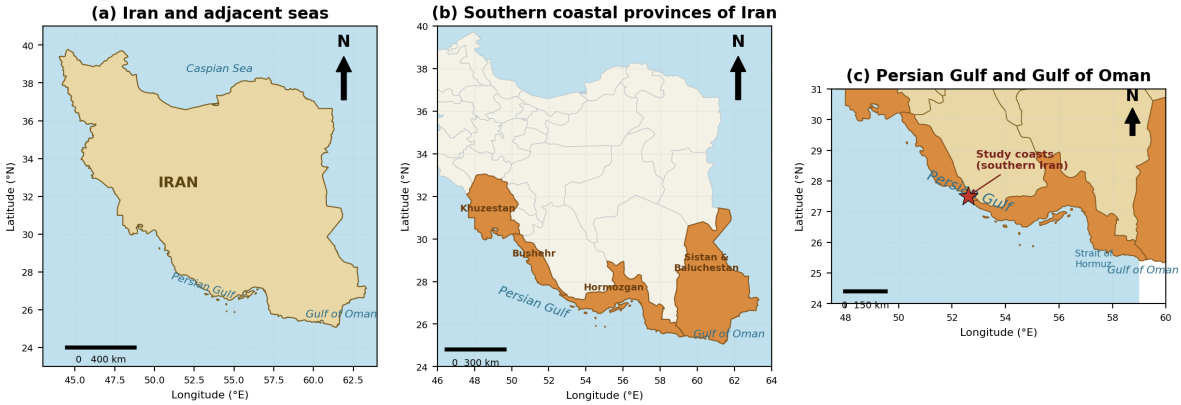

Figure 1: Study area: (a) Iran and its adjacent seas; (b) the southern coastal provinces of Iran; (c) the Persian Gulf and Gulf of Oman (base data: Natural Earth; authors' elaboration).

One of the primary challenges in coastal development is selecting an appropriate method to protect coastal areas, ports and marine waterways with minimal cost and minimal adverse impact on adjacent areas and coastlines. Water circulation near the shore is critically important for maintaining ecosystem health in ports and waterways: facilitating natural water exchange between the sea and the harbour can reduce pollution and its detrimental effects. Various structures exist for coastal protection artificial beaches, breakwaters, seawalls, groynes and offshore breakwaters among which breakwaters are the most important and widely used. To prevent water stagnation within ports, porous, perforated and slotted breakwaters without closed end walls (for example, spaced piles, slotted walls or submerged plates) can be arranged in single or multiple rows, causing minimal disruption to the natural sediment-transport cycle (Huang et al., 2011; Elsheikh et al., 2022). Unlike conventional impermeable breakwaters, which alter sediment-transport patterns, permeable breakwaters do not cause downstream erosion within the port area nor lead to sediment accumulation upstream. Their additional advantages include allowing fish passage, enabling natural sediment movement through the structure, suitability for relatively deep water, applicability where working space is limited, and reduced construction costs in deep water. Perforated breakwaters are constructed from recycled materials primarily because they consume a significantly lower volume of raw material and their design is simple and clear; they can be produced in various dimensions to suit the specific characteristics of each region (Yoon et al., 2018; Corbau et al., 2023). The use of recycled materials in breakwater construction is an innovative and sustainable approach that can yield significant environmental and economic benefits. A key advantage is the rapid speed of construction and installation. By shifting towards this type of breakwater, quarries can be conserved and preserved for future generations;

the utilisation of quarries should be carried out with careful planning and resource efficiency, and these breakwaters contribute significantly to that goal (Moradi & Shahnoori, 2021). This paper investigates the performance of permeable perforated breakwaters a new generation of breakwaters constructed from recycled materials. The structure is composed of a cubic box whose internal fill also consists of recycled materials, such as bottles. Two arrangement configurations are evaluated: single-row and double-row layouts with spacing. To enhance performance, regular holes are incorporated on both the front and rear faces; their function is to dissipate wave energy, with their number and diameter depending on environmental, hydraulic and structural variables. The weight of the structure relative to its volume is very low, and the amount of material used is minimal. The breakwater is categorised into submerged and non-submerged types, both examined here, and is anchored to the seabed using steel ballast or other methods (Zhao et al., 2019).

Many physical systems can be constructed and tested at small scale before being deployed in their actual environment; this is the best available approach, both economically and technically, for designing floating, submerged and immersed marine structures. A crucial requirement is adherence to the governing laws of modelling. In this context, the Froude number is primarily used for problems related to sea waves and the hydraulic similarity of floating bodies, while the Reynolds number is employed for problems concerning fluid flow. Although Reynolds similarity is also valid for floating bodies, it is not used in modelling such structures because it is impossible to build a model that operates at a speed significantly higher than the prototype (Asadian Ghahfakhari, 2006). Nowadays, numerical and laboratory simulations play a crucial role in predicting the forces acting on floating or fixed structures before their construction (Soltani & Aghtoman, 2004).

Against this background, the objective of this study is to analyse, through systematic physical-model experiments, the hydrodynamic behaviour of perforated breakwaters made from recycled materials under regular waves, and to determine how the arrangement, perforation percentage and perforation diameter govern wave run-up, transmission, reflection, uplift and stability thereby identifying the configuration that offers the best balance between wave attenuation and structural stability. The remainder of the paper reviews related studies, details the theoretical background and experimental methodology, presents and discusses the results, and finally draws conclusions.

MATERIALS AND METHODS

Floating and permeable breakwaters have been studied extensively. McCartney investigated the advantages and disadvantages of floating breakwaters of various configurations (McCartney, 1985). Kee conducted studies on the influence of porous members on wave–structure interaction and on the performance of double porous floating breakwaters using a multi-domain boundary-element method, concluding that optimal performance occurs at high wave frequencies (Kee, 2005). Koutandos and colleagues performed laboratory studies on box-type floating breakwaters under regular and irregular waves, examining the effect of incident-wave characteristics and geometric parameters such as width and draft (Koutandos et al., 2004). Dong and colleagues tested single, double and grillage-deck breakwaters under regular waves with and without current, identifying the grillage-deck type as suitable owing to its simplicity and cost-effectiveness (Dong et al., 2008).

Ozeren investigated wave transmission, reflection and breaking coefficients for tubular floating breakwaters with various mooring systems and found that pile moorings result in less wave transmission (Ozeren, 2009). Peña and colleagues reported laboratory results for floating breakwaters of four geometries, including a 1:15 physical prototype of the Port of Bayona break-

water and catamaran-shaped (π-shaped) forms (Peña et al., 2011). Teh and colleagues studied surface-piercing semi-cylindrical breakwaters of varying porosity under irregular waves (Teh et al., 2012). Mahmuddin and Kashiwagi combined a genetic algorithm with the boundary-element method to design optimised, high-efficiency floating breakwaters across a wide frequency range (Mahmuddin & Kashiwagi, 2014), and, in Iran, Taheri, Kolahdoozan and colleagues used physical modelling to evaluate stepped floating breakwaters and compare them with a π-shaped form of equal width and draft (Taheri et al., 2014). Dhinakaran investigated the hydrodynamic characteristics of perforated, shoreward semi-circular breakwaters under irregular waves, analysing reflection, run-up, transmission, forces and pressures (Dhinakaran et al., 2008).

More recent work has advanced both the understanding and the sustainability of permeable breakwaters. Experimental and numerical studies have clarified wave transmission, reflection and forces on perforated and slotted structures (Xu et al., 2022; Yang et al., 2024; Liu et al., 2023; Peng et al., 2023; Zhang et al., 2022), while comparative and formula-assessment studies have refined transmission predictions for submerged, slotted and low-crested breakwaters (Brancasi et al., 2022; Hassanpour et al., 2023; Koraim, 2011). Perforated caissons and breakwater-integrated devices have been examined for wave-force mitigation and multifunctional use (Ko et al., 2024; Lee et al., 2020; Zhao et al., 2019; Wang et al., 2025), and the use of recycled and eco-friendly materials in marine construction has been increasingly documented (Kenny & Rozovsky, 2023; Corbau et al., 2023; Moradi & Shahnoori, 2021). The foundational theory of wave reflection and transmission at permeable breakwaters remains a common reference point (Sollitt & Cross, 1972). Collectively, these studies motivate the present physical-model investigation of perforated breakwaters built from recycled materials.

Given the vast extent of Iran's coastline more than 2,700 km (657 km along the southern Caspian Sea, 784 km along the Gulf of Oman and 1,259 km along the Persian Gulf)—the need for a correct and scientific design methodology for coastal-protection structures is evident. In this study, physical models of perforated breakwaters with various configurations (single-row, double-row, double-sided, horizontal and vertical) were tested in a wave flume, and the reflection coefficient, run-up, transmission coefficient, uplift force and overturning moment were measured. Lightweight, durable recycled materials were used to construct the models.

Wave theory and governing relations

Three relative-depth regimes are distinguished on the basis of the ratio d/L: shallow water when $d/\lambda < 1/20$; intermediate water when $1/20 < d/\lambda < 1/2$; and deep water when $d/\lambda > 1/2$ (Ministry of Roads and Transportation, 2006). The trajectory of water-particle motion in progressive waves at different relative depths is illustrated in Figures 2 and 3. (Fig. 2 and 3)

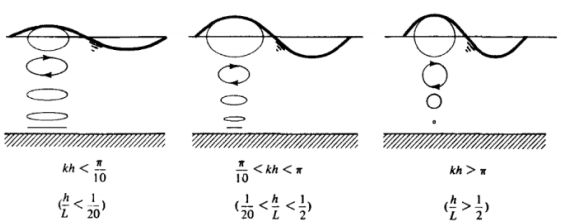

Figure 2: Path of water-particle motion in progressive waves at different relative depths (Ippen, 1966)

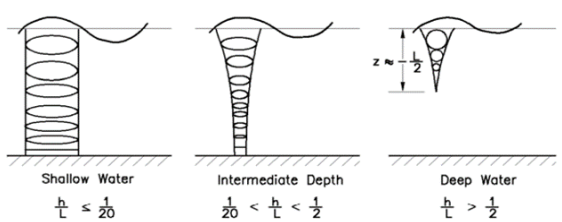

Figure 3: General schematic of the water-particle motion path (Ippen, 1966)

The period T and wave height H are the identifying indices of surface water waves. In generating waves with a wave-maker, two parameters must be controlled: the speed of the piston or paddle, and the spatial range of its forward and backward stroke. In practice, wave generation is constrained by the limited speed of the paddle and by the nature of waves, which leads to instability and breaking (wave steepness in deep water and relative height in shallow water) (Asadian Ghahfakhari, 2006). Ippen presented a clear illustration of the water-particle trajectory: in deep water the influence of the orbital circles extends to half the wavelength, in shallow water the circle diameter remains essentially unchanged to the seabed, and in intermediate water the diameter near the seabed is smaller than at the surface (Ippen, 1966). The dispersion relation and the derived wavelength and celerity take limiting forms in each regime. In shallow water:

$$\omega^2 = g\,k\tanh(kd) = g\,k^2\,d \quad (1)$$

$$L = (gT^2/2\pi)\tanh(2\pi d/L) \rightarrow L = T\sqrt{(gd)} \quad (2)$$

$$C^2 = (L^2/T^2)\,kd = gk \rightarrow C = \sqrt{(gd)} \quad (3)$$

Thus, in shallow water the wavelength depends on the wave period and the water depth, and the propagation speed is determined solely by the depth. In deep water, since kd is large, tanh(kd) approaches unity:

$$\omega^2 = g\,k\tanh(kd) \approx g\,k \quad (4)$$

$$L_0 = gT^2/2\pi\,,\quad C_0 = gT/2\pi \quad (5)$$

For wave breaking, Miche proposed a limiting steepness valid at any depth (Miche, 1944):

$$(H/L)_max = (1/7)\tanh(2\pi d/L) \quad (6)$$

In deep water this reduces to (H_0/L_0) _max = 1/7, so the maximum wave height is limited to one-seventh of the wavelength; in shallow water it reduces to a depth-limited form, so that wave height is limited by the water depth. Consequently, the further a structure extends seaward, the larger and more destructive the waves it must withstand. A summary of linear wave theory and wave characteristics is given in Table 1. (Tab. 1)

Table 1: Summary of linear wave theory and wave characteristics for shallow, intermediate and deep water

Relative Depth	Shallow Water $\frac{d}{L} < \frac{1}{25}$	Transitional Water $\frac{1}{25} < \frac{d}{L} < \frac{1}{2}$	Deep Water $\frac{d}{L} > \frac{1}{2}$
1. Wave profile	Same As >	$\eta = \frac{H}{2}\cos\left[\frac{2\pi x}{L} - \frac{2\pi t}{T}\right] = \frac{H}{2}\cos\theta$	< Same As
2. Wave celerity	$C = \frac{L}{T} = \sqrt{gd}$	$C = \frac{L}{T} = \frac{gT}{2\pi}\tanh\left(\frac{2\pi d}{L}\right)$	$C = C_0 = \frac{L}{T} = \frac{gT}{2\pi}$
3. Wavelength	$L = T\sqrt{gd} = CT$	$L = \frac{gT^2}{2\pi}\tanh\left(\frac{2\pi d}{L}\right)$	$L = L_0 = \frac{gT^2}{2\pi} = C_0 T$
4. Group velocity	$C_g = C = \sqrt{gd}$	$C_g = nC = \frac{1}{2}\left[1 + \frac{4\pi d/L}{\sinh(4\pi d/L)}\right]C$	$C_g = \frac{1}{2}C = \frac{gT}{4\pi}$
5. Water particle velocity (a) Horizontal	$u = \frac{H}{2}\sqrt{\frac{g}{d}}\cos\theta$	$u = \frac{H}{2}\frac{gT}{L}\frac{\cosh[2\pi(z+d)/L]}{\cosh(2\pi d/L)}\cos\theta$	$u = \frac{\pi H}{T}e^{\left(\frac{2\pi z}{L}\right)}\cos\theta$
(b) Vertical	$w = \frac{H\pi}{T}\left(1 + \frac{z}{d}\right)\sin\theta$	$w = \frac{H}{2}\frac{gT}{L}\frac{\sinh[2\pi(z+d)/L]}{\cosh(2\pi d/L)}\sin\theta$	$w = \frac{\pi H}{T}e^{\left(\frac{2\pi z}{L}\right)}\sin\theta$

6. Water particle accelerations (a) Horizontal	$a_x = \frac{H\pi}{T}\sqrt{\frac{g}{d}}\sin\theta$	$a_x = \frac{g\pi H}{L}\frac{\cosh[2\pi(z+d)/L]}{\cosh(2\pi d/L)}\sin\theta$	$a_x = 2H\left(\frac{\pi}{T}\right)^2 e^{\left(\frac{2\pi z}{L}\right)}\sin\theta$
(b) Vertical	$a_z = -2H\left(\frac{\pi}{T}\right)^2\left(1-\frac{z}{d}\right)\cos\theta$	$a_z = -\frac{g\pi H}{L}\frac{\sinh[2\pi(z+d)/L]}{\cosh(2\pi d/L)}\cos\theta$	$a_z = -2H\left(\frac{\pi}{T}\right)^2 e^{\left(\frac{2\pi z}{L}\right)}\cos\theta$
7. Water particle displacements (a) Horizontal	$\xi = -\frac{HT}{4\pi}\sqrt{\frac{g}{d}}\sin\theta$	$\xi = -\frac{H}{2}\frac{\cosh[2\pi(z+d)/L]}{\sinh(2\pi d/L)}\sin\theta$	$\xi = -\frac{H}{2}e^{\left(\frac{2\pi z}{L}\right)}\sin\theta$
(b) Vertical	$\zeta = \frac{H}{2}\left(1-\frac{z}{d}\right)\cos\theta$	$\zeta = \frac{H}{2}\frac{\sinh[2\pi(z+d)/L]}{\sinh(2\pi d/L)}\cos\theta$	$\zeta = \frac{H}{2}e^{\left(\frac{2\pi z}{L}\right)}\cos\theta$
8. Subsurface pressure	$p = \rho g(\eta - z)$	$p = \rho g\eta\frac{\cosh[2\pi(z+d)/L]}{\cosh(2\pi d/L)} - \rho g z$	$p = \rho g\eta e^{\left(\frac{2\pi z}{L}\right)} - \rho g z$

Breakwater types and floating-body mechanics

Breakwaters are generally classified as sloped (rubble-mound), vertical, composite and floating types. A floating body remains buoyant at the surface and is permitted to move within a specific range; its design must satisfy both performance and safety requirements (Coastal Structures Design Guideline, 2013). Mooring systems comprising mooring lines, anchors, winches, sinkers, buoys, rods, shackles and fenders strongly influence the motions of a floating body. Mooring methods include catenary (slack), taut and dolphin-type bracing; in taut bracing (e.g., the tension-leg platform) the lines carry large initial tension so that motions and footprint are minimised, at the cost of high line forces (Fig. 4).

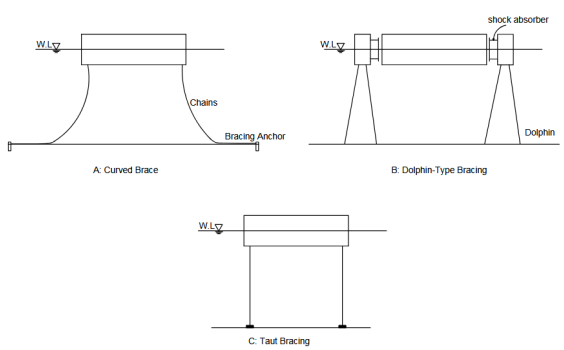

Figure 4: Representative bracing (mooring) techniques for a floating body

When port facilities are built as floating structures, the design must account for wind drag, current drag, wave excitation, wave drift, wave-making resistance, restoring force and mooring force (Coastal Structures Design Guideline, 2013). The forces on a floating breakwater are commonly resolved into a hydrodynamic force (from lateral and vertical wave pressures, dependent on geometry, wave height and wind speed) and a displacement force (from the change in water mass as waves pass through the structure). If the body is treated as rigid, its motion has six degrees of freedom—surge, sway, heave, roll, pitch and yaw (Fig. 5).

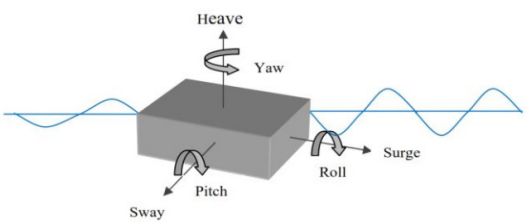

Figure 5: Degrees of freedom of a floating body's motion (after Coastal Structures Design Guideline, 2013)

The displacement of a breakwater under wave forces is obtained by first computing the hydrostatic and hydrodynamic forces, then the acceleration from Newton's second law, and finally the displacement from the equation of motion:

$$a = F_total / m \quad (14)$$
$$x = x_0 + v_0 t + \tfrac{1}{2} a t^2 \quad (15)$$
$$F_W = \tfrac{1}{2} \cdot \rho \cdot C_M \cdot A \cdot a \quad (16)$$

where a is acceleration, F_total the total force, m the mass, x the displacement, v_0 the initial velocity, F_W the wave force (Morison's equation for submerged bodies), ρ the water density, C_M the added-mass coefficient, and A the wave-impact area. For stability, Van der Meer classified rubble-mound structures using the stability parameter H/(ΔD), where Δ = (ρ_r/ρ_w − 1) is the relative buoyant density and D the characteristic dimension (Van der Meer, 1992). Structures with H/(ΔD) < 1 (e.g., caissons, seawalls) permit no damage; 1–4 corresponds to stable breakwaters; 3–6 to flexible berm/S-shaped breakwaters; 6–20 to gravel slopes; 15–500 to sandy beaches; and > 500 to silty beaches.

Perforated breakwaters from recycled materials

To enhance performance, regular perforations are incorporated on the front and rear faces of the recycled units (bottles); their function is to dissipate wave energy, with number and diameter depending on environmental, hydraulic and structural variables. The structure is very light relative to its volume, uses minimal material, and may be submerged or non-submerged; it is anchored to the seabed with steel ballast or other means. A schematic of the recycled-material (bottle) arrangement is shown in Figure 6. (Fig. 6)

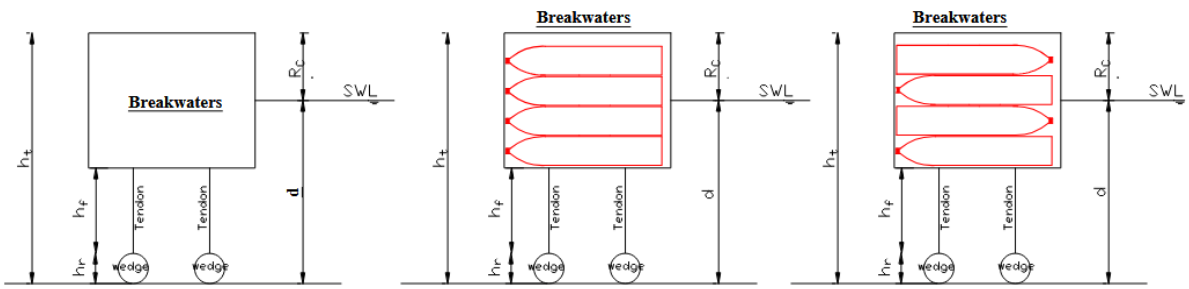

Figure 6: Schematic of the recycled-material (bottle) arrangement of the perforated breakwater (after Yoon et al., 2018).

The principal advantages of this structure include reduced wave reflection and partial energy dissipation as waves pass through the perforations; easier and more cost-effective installation than fixed breakwaters; the generation of vortices and turbulence behind the structure that further reduce wave energy; prefabrication with no in-situ concrete casting; the possibility of re-floating and relocation; a more pleasing appearance; and simpler maintenance. Its efficiency decreases as the ratio of wavelength to structure length increases, so wave attenuation is less effective for longer wavelengths (Yoon et al., 2018; Huang et al., 2011).

Governing design variables

Environmental variables describe the wave boundary conditions: wave height at the toe H (the significant height H_s for irregular waves), wave period T (mean T_m and peak T_p for irregular waves), wave steepness S, water depth d, and angle of attack β (Van der Meer, 1992). Wave steepness and the deep-water wavelength are:

$$S = 2\pi H / (gT^2) \quad (17)$$
$$L = gT^2 / (2\pi) \quad (18)$$

Hydraulic variables are the key responses governing hydraulic design wave run-up and run-down, overtopping, transmission and reflection. The transmission coefficient C_t and the reflection coefficient are defined as ratios of the transmitted (or reflected) to the incident characteristic wave height, or equivalently the square root of the corresponding energy ratio:

$$C_t = H_st / H_s = \sqrt{(E_t / E_i)} \quad (19)$$

$$C_r = H_r / H_i = \sqrt{(E_r / E_i)} \quad (20)$$

Structural variables relate the structure to the wave field through the stability number and relative buoyant density:

$$N_s = H / (\Delta D) \quad (21)$$

$$\Delta = (\rho_r / \rho_w) - 1 \quad (22)$$

The cross-sectional structural variables of the perforated breakwater water depth d, total height h_t, water height above the wedge h_f, freeboard R_c, wedge height h_r, breakwater radius R_s and porosity P are illustrated in Figure 7. As porosity increases, the force on the structure decreases; porosity can be tuned to optimise both the hydraulic responses and the forces on the structure. (Fig. 7)

Experimental set-up

The variables governing the assessment of hydraulic performance are summarised in Table 2; all procedures and analyses were conducted accordingly. To ensure order and accuracy, a structured test matrix was prepared: for each breakwater, one wave height was tested for each wave period, and on completion the next breakwater was placed in the flume. The complete matrix of wave tests is given in Table 3, and the model-naming abbreviations follow the table.

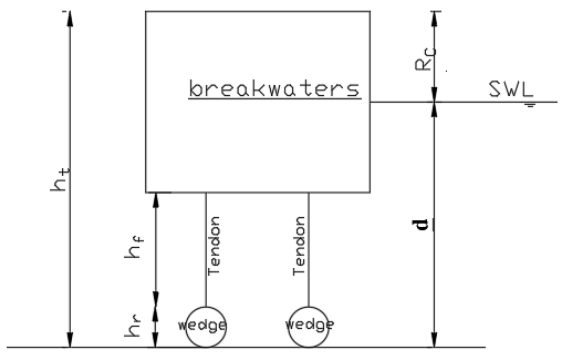

Figure 7: Governing variables of the structural cross-section of the perforated breakwater (Miche, 1944).

Table 2: Governing variables in the hydraulic-performance evaluation

Variable	Symbol	Value in the model
Wave height	H	23 cm
Wave period	T	1.012 s
Water depth at the structure	d	80 cm
Wave steepness	H/λ	0.142
Relative depth	d/λ	0.5
Water depth to wave height ratio	d/H	3.478
Piston-type wave-maker stroke	S	14.55 cm
Wave frequency	f	0.988 Hz
Scale	–	1:13

Table 3: Matrix of wave tests on the breakwater models

NO	Type	L_B (cm)	D_B (cm)	H_B (cm)	λ (cm)	T (s)	H (cm)	h_r (cm)	h_f (cm)	h_r/h_f	x
1	CBOWFW1	250	30	60	160	1.012	23	10	70	0.143	12
4	HBOWFW4	250	30	60	160	1.012	23	10	40	0.25	11
5	HBOWEW5	250	30	60	160	1.012	23	10	40	0.25	10
6	HBOWFEW6	250	30	60	160	1.012	23	10	40	0.25	10.5
10	CBOWSW10	250	triangle	60	160	1.012	23	10	70	0.143	15.5
12	HBOWSW12	250	triangle	60	160	1.012	23	10	40	0.25	14.5
13	HBOWSW13	250	triangle	60	160	1.012	23	10	40	0.25	13.5

15	HBOWSW15	250	triangle	60	160	1.012	23	10	40	0.25	12.5
16	CBOWFW16	300	30	60	160	1.012	23	10	70	0.143	12
19	HBOWFW19	300	30	60	160	1.012	23	10	40	0.25	11.5
20	HBOWEW20	300	30	60	160	1.012	23	10	40	0.25	10.5
21	HBOWFEW21	300	30	60	160	1.012	23	10	40	0.25	11
25	CBOWFW25	250	60	60	160	1.012	23	10	70	0.143	12
27	CBOWFEW27	250	60	60	160	1.012	23	10	70	0.143	12
28	HBOWFW28	250	60	60	160	1.012	23	10	40	0.25	11
29	HBOWEW29	250	60	60	160	1.012	23	10	40	0.25	10
30	HBOWFEW30	250	60	60	160	1.012	23	10	40	0.25	10.5

Model-naming key: CBOWFW – complete breakwater on the water, both bottle sides closed, first side facing the wave; CBOWEW as above but the end facing the wave; CBOWFEW – as above but the middle facing the wave; HBOWEW half of the breakwater on the water, bottle top closed and bottom open, bottom facing the wave; HBOWFEW half of the breakwater on the water in a combined open/closed arrangement facing the wave; the trailing S denotes a triangular (sloped) end arrangement.

FINDINGS AND DISCUSSION

The physical-model tests yielded the following general results:

•The perforations effectively dissipated wave energy.

•The horizontal breakwaters near the water surface exhibited lower uplift forces than the other models.

•The two-row, double-sided configuration in the combined wave-facing condition showed minimal displacement and the highest stability.

•Increasing the number or diameter of the perforations directly reduced the reflection and transmission coefficients.

Effect of perforation percentage on wave run-up

For breakwaters with an open (wave-facing) front and a closed rear, the run-up on the impermeable models (CBOWFW16, CBOWSW10, CBOWFW1, CBOWFW25) was compared with that on four single-side perforated models (HBOWFW4, HBOWFW12, HBOWFW19, HBOWFW28). The run-up was higher on the impermeable breakwater and sometimes led to overtopping. Introducing perforations covering up to 7% of the exposed surface reduced the run-up, because the perforations dissipate energy so that less energy remains for run-up. Displacements of the four perforated models were nearly identical; the optimal 7%-perforation case was HBOWFW28 (Fig. 8, a–d).

Effect of perforation size on wave run-up

The run-up on breakwaters with larger perforation diameters exceeded that with medium diameters, and the run-up with smaller diameters also exceeded that with medium diameters; the medium (composite) perforation size therefore performed best, owing to greater energy dissipation and reduced run-up. Furthermore, increasing the d/L ratio and thus decreasing the wavelength and wave period reduced the run-up (Fig. 9, a–c).

Advantages of recycled-material breakwaters

The application of recycled materials in breakwater construction offers several engineering and environmental advantages: it establishes a controlled hydraulic connection between the open sea and the harbour basin, promoting natural water exchange, improving water quality and reducing corrosion from stagnation; it lowers the environmental footprint and material-procurement cost (subject to proper characterisa-

tion of the recycled material's geotechnical and durability properties); it minimises interference with littoral drift, reducing downdrift erosion and updrift accretion; it enhances ecological connectivity by allowing fish passage; it suits constrained and moderately deep sites; it shortens the construction schedule; it attenuates run-up and overtopping; it lowers hydrodynamic loading and the risk of toe scour; and the phase lag between forces on the front and rear perforated faces improves hydrodynamic stability. The long-term behaviour of recycled materials nevertheless depends strongly on the source material and environmental exposure, so rigorous physical and numerical modelling remains indispensable for validation and optimisation (Kenny & Rozovsky, 2023; Corbau et al., 2023).

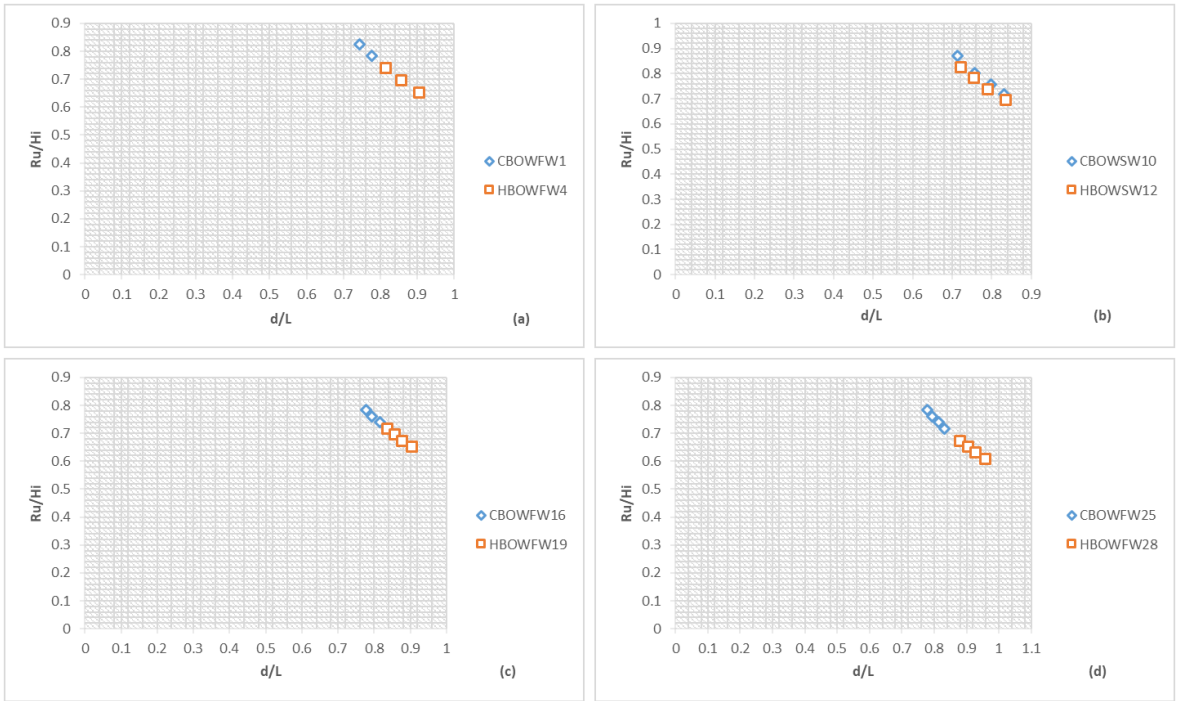

Figure 8: Effect of the perforation percentage on the relative wave run-up (Ru/Hi) versus relative depth (d/L) for single-side (wave-facing) perforated breakwaters, for four model pairs (a–d)

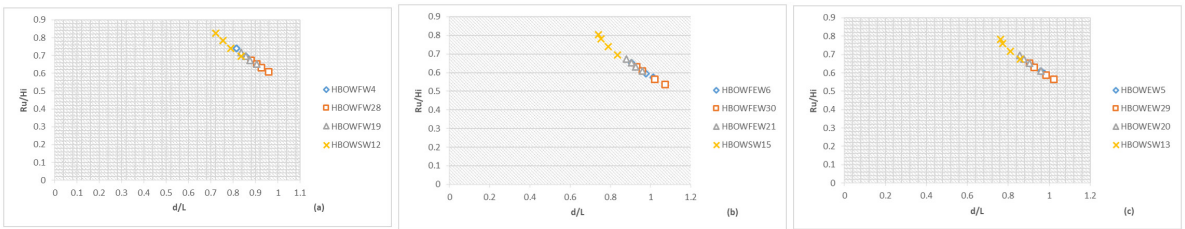

Figure 9: Effect of the perforation diameter on the relative wave run-up for single-side perforated breakwaters (a–c)

RESULTS AND CONCLUSION

The findings demonstrate that structural geometry and configuration exert a predominant influence on hydrodynamic performance. Perforated breakwaters not only provided effective wave-energy dissipation but, through the incorporation of recycled materials, also offered a sustainable and economically viable solution for

coastal protection. This synergy between optimised hydraulic design (through perforations) and sustainable material use establishes a promising pathway for eco-efficient maritime infrastructure. The observed reduction of run-up and transmission with moderate perforation, and its partial reversal at very high porosity, is consistent with recent experimental and numerical studies showing that an intermediate porosity maximises energy dissipation while limiting transmission (Xu et al., 2022; Yang et al., 2024; Elsheikh et al., 2022). The superior stability of the two-row, double-sided arrangement accords with the phase-lag mechanism reported for perforated caissons and multi-row permeable structures (Liu et al., 2023; Peng et al., 2023; Huang et al., 2011). Scale effects associated with viscous flow through the perforations should, however, be borne in mind when transferring the laboratory results to prototype scale (Sollitt & Cross, 1972; Brancasi et al., 2022).

Wave run-up

•In single-side perforated breakwaters (seaward face), increasing the perforation percentage up to 42.78% reduced the wave run-up.

•Increasing the perforation percentage further to 78.5% reversed the trend and slightly increased run-up, although it remained lower than that of HBOWFEW27.

•In double-side perforated breakwaters, increasing the perforation percentage reduced the run-up.

•The optimal cases for reducing run-up and displacement were HBOWFW4 and HBOWFW28 at 7% perforation, HBOWFEW6 and HBOWFEW30 at 42.78%, and HBOWEW5 and HBOWEW29 at 78.5%.

Wave transmission

•Increasing the perforation percentage increased wave transmission through the structure: the 7%-perforation breakwater had the highest, and the 42.78%-perforation breakwater the lowest, transmission coefficient; the optimal case for minimising transmission was therefore the 42.78%-perforation breakwater.

•Increasing the perforation percentage from 7% to 42.78% increased wave-energy dissipation, whereas increasing it from 42.78% to 78.5% decreased dissipation.

•Overall, the two-row, double-sided perforated breakwater in the combined wave-facing arrangement provided the best balance of wave attenuation and stability, confirming perforated breakwaters made from recycled materials as an effective, sustainable coastal-protection option.

REFERENCES

Asadian Ghahfakhari, M. (2006). Design and construction of a wave-maker for a marine laboratory (Master's thesis). Sharif University of Technology, Faculty of Mechanical Engineering; 9th Marine Industries Conference, Noor, Mazandaran. [in Persian]

Brancasi, A., Leone, E., Francone, A., Scaravaglione, G., & Tomasicchio, G. R. (2022). On formulae for wave transmission at submerged and low-crested breakwaters. Journal of Marine Science and Engineering, 10(12), 1986. https://doi.org/10.3390/jmse10121986

Coastal Engineering Manual (CEM). (2005). Coastal engineering manual. U.S. Army Corps of Engineers (USACE), Washington, DC.

Chegini, V. (1998). Wave theories (Marine Engineering Books Collection No. 1). Jihad Water and Watershed Research Company, 301 pp. [in Persian]

Coastal Structures Design Guideline. (2013). Part II: Design conditions (Publication No. 631, Chapter 8).

Coastal Structures Design Manual. (2013). Part 7: Port protection facilities – floating breakwater (p. 557).

Corbau, C., Nardin, W., Vaccaro, C., Vona, I., & Simeoni, U. (2023). Experimental design and field deployment of an artificial bio-reef produced by mollusk shell recycling. Marine Environmental Research, 183, 105833. https://doi.org/10.1016/j.marenvres.2022.105833

Dean, R. G., & Dalrymple, R. A. (2000). Water wave

mechanics for engineers and scientists. World Scientific, Singapore.

Dhinakaran, G., Sundar, V., Sundaravadivelu, R., & Graw, K. U. (2008). Hydrodynamic characteristics of seaside perforated semicircular breakwaters due to random waves. Journal of Waterway, Port, Coastal, and Ocean Engineering, 134(4), 237–251.

Dong, G.-H., Zheng, Y.-N., Li, Y.-C., Teng, B., Guan, C.-T., & Lin, D.-F. (2008). Experiments on wave transmission coefficients of floating breakwaters. Ocean Engineering, 35(8–9), 931–938.

Elsheikh, A. K., Mostafa, Y. E., & Mohamed, M. M. (2022). A comparative study between some different types of permeable breakwaters according to wave energy dissipation. Ain Shams Engineering Journal, 13(4), 101646. https://doi.org/10.1016/j.asej.2021.11.015

Hassanpour, N., Vicinanza, D., & Contestabile, P. (2023). Determining wave transmission over rubble-mound breakwaters: Assessment of existing formulae through benchmark testing. Water, 15(6), 1111. https://doi.org/10.3390/w15061111

Huang, Z., Li, Y., & Liu, Y. (2011). Hydraulic performance and wave loadings of perforated/slotted coastal structures: A review. Ocean Engineering, 38(10), 1031–1053. https://doi.org/10.1016/j.oceaneng.2011.03.002

Ippen, A. T. (1966). Estuary and coastline hydrodynamics. McGraw-Hill, New York.

Kee, S. T. (2005). Performance evaluation of submerged dual buoy/porous-membrane breakwaters. KSCE Journal of Civil Engineering, 9(4), 279–287.

Kenny, A., & Rozovsky, E. O. (2023). Six-year-old ecological concrete in a marine environment: A case study. Sustainability, 15(18), 13780. https://doi.org/10.3390/su151813780

Ko, C.-H., Fan, C.-Y., & Tsai, C.-P. (2024). Experimental investigation of wave pressure on breakwater-integrated oscillating water column devices with a perforated wall. Journal of Marine Science and Engineering, 12(10), 1782. https://doi.org/10.3390/jmse12101782

Koraim, A. S. (2011). Hydrodynamic characteristics of slotted breakwaters under regular waves. Journal of Marine Science and Technology, 16(3), 331–342.

Koutandos, E. V., Karambas, T. V., & Koutitas, C. G. (2004). Floating breakwater response to wave action using a Boussinesq model coupled with a 2DV elliptic solver. Journal of Waterway, Port, Coastal, and Ocean Engineering, 130(5), 243–255.

Lee, B. W., Jung, J.-S., Park, W.-S., & Yoon, J.-S. (2020). Wave force characteristics and stability of detached breakwaters consisting of open cell caissons interlocked via crushed stones. Water, 12(10), 2873. https://doi.org/10.3390/w12102873

Liu, X., Liu, Y., Lin, P., & Wang, D. (2023). Experimental and numerical studies of solitary wave interaction with perforated caisson breakwaters. Physics of Fluids, 35(5), 057119. https://doi.org/10.1063/5.0149420

Mahmuddin, F., & Kashiwagi, M. (2014). Performance evaluation of an optimized floating breakwater in oblique waves with a higher-order boundary element method. Applied Mechanics and Materials, 493, 205–210.

McCartney, B. L. (1985). Floating breakwater design. Journal of Waterway, Port, Coastal, and Ocean Engineering, 111(2), 304–318.

Miche, M. (1944). Mouvement ondulatoire des mers en profondeur constante ou décroissante. Annales des Ponts et Chaussées, 114, 25–78.

Ministry of Roads and Transportation. (2006). Iranian code of practice for the design of ports and marine structures – Bulletin 300: Breakwaters and coastal-protection structures (364 pp.). Tehran. [in Persian]

Moradi, S., & Shahnoori, S. (2021). Eco-friendly mix for roller-compacted concrete: Effects of Persian-Gulf-dredged marine sand on durability and resistance parameters of concrete. Construction and Building Materials, 281, 122555. https://doi.org/10.1016/j.conbuildmat.2021.122555

Ozeren, Y. (2009). Experimental and numerical investigations of floating breakwater performance

(Doctoral dissertation). The University of Mississippi, USA.

Peña, E., Ferreras, J., & Sanchez-Tembleque, F. (2011). Experimental study on wave transmission coefficient, mooring lines and module connector forces with different designs of floating breakwaters. Ocean Engineering, 38(10), 1150–1160.

Peng, J., Li, K., Gu, S., & Cong, Y. (2023). Numerical simulation of the interaction between waves and pile breakwater with horizontal slotted plates. Ocean Engineering, 287, 115777. https://doi.org/10.1016/j.oceaneng.2023.115777

Sollitt, C. K., & Cross, R. H. (1972). Wave transmission through permeable breakwaters. Coastal Engineering Proceedings, 1(13), 1827–1846. https://doi.org/10.1061/9780872620490.106

Soltani, M., & Aghtoman, P. (2004). Wave forces on marine structures. Marine engineering references. [in Persian]

Taheri, O., Kolahdoozan, M., & Bali, M. (2014). Experimental evaluation of the energy-transmission coefficient for stepped floating breakwaters. Journal of Marine Engineering, 10(19), 47–58. [in Persian]

Teh, H. M., Venugopal, V., & Bruce, T. (2012). Hydrodynamic characteristics of a free-surface semicircular breakwater exposed to irregular waves. Journal of Waterway, Port, Coastal, and Ocean Engineering, 138(2), 149–163.

Van der Meer, J. W. (1992). Conceptual design of rubble-mound breakwaters. In Proceedings of the short course on the design and reliability of coastal structures, 23rd International Conference on Coastal Engineering, Venice (pp. 447–510). ASCE, New York.

Wang, Y. Z., Ji, C. Y., Xu, S., et al. (2025). Theoretical study on the wave attenuation performance of floating breakwater with a rectangular cross-section. China Ocean Engineering, 39(2), 244–255. https://doi.org/10.1007/s13344-025-0034-5

Xu, W., Chen, C., Htet, M. H., Sarkar, M. S. I., Tao, A., Wang, Z., Fan, J., & Jiang, D. (2022). Experimental investigation on Bragg resonant reflection of waves by porous submerged breakwaters on a horizontal seabed. Water, 14(17), 2682. https://doi.org/10.3390/w14172682

Yang, S., Yang, L., Shi, B., Na, J., & Guo, Y. (2024). Experimental investigation on wave dissipation of perforated pipe breakwater under regular wave conditions. Journal of Marine Science and Engineering, 12(12), 2137. https://doi.org/10.3390/jmse12122137

Yoon, J.-S., Ha, T., & Jung, J. (2018). Laboratory experiments on characteristics of perforated-type floating breakwaters. Journal of Coastal Research, Special Issue 85, 1051–1055.

Zhang, B., Wang, X. Y., Zhao, Y., Liu, Y., & Jin, H. (2022). Numerical study of wave interactions with a new pile-supported curtain wall breakwater. Ocean Engineering, 265, 112431. https://doi.org/10.1016/j.oceaneng.2022.112431

Zhao, X. L., Ning, D. Z., & Zou, Q. (2019). Hybrid floating breakwater-WEC system: A review. Ocean Engineering, 186, 106126. https://doi.org/10.1016/j.oceaneng.2019.106126

COPYRIGHTS

©2023 The author(s). This is an open access article distributed under the terms of the Creative Commons Attribution (CC BY 4.0), which permits unrestricted use, distribution, and reproduction in any medium, as long as the original authors and source are cited. No permission is required from the authors or the publishers.

HOW TO CITE THIS ARTICLE

Ahmadi,J , Hadi Tavana,M , Delavari,E and Basirat,S . (2025). Laboratory Analysis of the Hydrodynamic Behavior of Perforated Breakwaters Constructed from Recycled Materials. International Journal of Urban Management and Energy Sustainability, 6(4), 353-365.

DOI: 10.22034/ijumes.2026.2097984.1396